A Solution Processable High-Performance Thermoelectric Copper Selenide Thin Film

Zhaoyang Lin, Courtney Hollar, Joon Sang Kang, Anxiang Yin, Yiliu Wang, Hui-Ying Shiu, Yu Huang, Yongjie Hu, Yanliang Zhang,* and Xiangfeng Duan**

A solid-state thermoelectric device is attractive for diverse technological areas such as cooling, power generation and waste heat recovery with unique advantages of quiet operation, zero hazardous emissions, and long lifetime. With the rapid growth of flexible electronics and miniature sensors, the low-cost flexible thermoelectric energy harvester is highly desired as a potential power supply. Herein, a flexible thermoelectric copper selenide (Cu_2Se) thin film, consisting of earth-abundant elements, is reported. The thin film is fabricated by a low-cost and scalable spin coating process using ink solution with a truly soluble precursor. The Cu_2Se thin film exhibits a power factor of 0.62 mW/(m K^2) at 684 K on rigid Al_2O_3 substrate and 0.46 mW/(m K^2) at 664 K on flexible polyimide substrate, which is much higher than the values obtained from other solution processed Cu_2Se thin films (<0.1 mW/(m K^2)) and among the highest values reported in all flexible thermoelectric films to date (≈0.5 mW/(m K^2)). Additionally, the fabricated thin film shows great promise to be integrated with the flexible electronic devices, with negligible performance change after 1000 bending cycles. Together, the study demonstrates a low-cost and scalable pathway to high-performance flexible thin film thermoelectric devices from relatively earth-abundant elements.

Thermoelectric (TE) power conversion is a solid-state and environmentally friendly energy conversion technology with broad applications in cooling, power generation, and waste heat recovery.[1,2] The TE device exhibits many attractive features, including cleanness without noise or emission of any hazardous substance, high reliability, a long life time, safe and stable electricity output.[3,4] The thermoelectric efficiency of a given material is determined by the nondimensional figure of merit ZT, defined as $ZT = S^2\sigma T/\kappa$ where S, σ, κ, and T are the Seebeck coefficient, electrical conductivity, thermal conductivity, and absolute temperature, respectively. Considerable efforts have been devoted to improving the ZT by tailoring electron and phonon transport via nanostructuring in the past two decades.[5,6] Nanostructures can reduce the phonon thermal conductivity through interface scattering, while maintaining or even improving the electronic transport through quantum confinement or interface energy filtering.[7–11] Indeed, significant ZT enhancement has been realized in both thin film structures such as superlattices and nanostructured bulk (nanobulk) materials containing nanostructures in a bulk matrix.[12–18] Despite of considerable progresses to date, it remains a significant challenge to implement these approaches for large-scale commercialization due to the high material cost (e.g., using the expensive rare materials, Bi, Te, etc.) and complex fabrication processes.[19,20] With the rapid rise of miniature sensors and flexible electronics, flexible thermoelectric unit may offer an attractive solution for power supply.[21–26] To this end, a flexible thin film thermoelectric device based on low-cost earth-abundant elements is highly desired.

Copper selenide (Cu_2Se) has been receiving much attention as a promising thermoelectric material for its excellent thermoelectric performance and affordable cost.[27–30] The simple crystal structure and low cost of the starting material offer many exciting opportunities in industrial production. Liu et al. reported a "liquid-like" behavior of copper ions around a crystalline sublattice of Se, resulting in an intrinsically low lattice thermal conductivity, enabling an enhanced ZT of 1.5 at 1000 K in bulk Cu_2Se synthesized with vacuum melting followed by consolidation using spark plasma sintering.[27] Recently, a ZT of 1.6 at 973 K has been achieved by hot pressing Cu_2Se powder prepared from high-energy ball milling.[29] Importantly, both the Cu and Se are more abundant than Bi and Te, which could lead to a great cost reduction for practical applications. However, despite of the high performance realized in the bulk form, the Cu_2Se thin films usually exhibit a much lower

Dr. Z. Lin, Dr. A. Yin, Y. Wang, Prof. X. Duan
Department of Chemistry and Biochemistry
California NanoSystems Institute
University of California
Los Angeles, CA 90095, USA
E-mail: xduan@chem.ucla.edu
C. Hollar, Prof. Y. Zhang
Department of Mechanical and Biomedical Engineering
Boise State University
ID 83725, USA
E-mail: yanliangzhang@boisestate.edu
J. S. Kang, Prof. Y. Hu
Department of Mechanical and Aerospace Engineering
University of California
Los Angeles, CA 90095, USA
E-mail: yhu@seas.ucla.edu
H.-Y. Shiu, Prof. Y. Huang
Department of Materials Science and Engineering
California NanoSystems Institute
University of California
Los Angeles, CA 90095, USA

DOI: 10.1002/adma.201606662

thermoelectric performance, mainly due to structural imperfections, including voids and defects in the films.[31–33]

Herein, we report a high-performance flexible thermoelectric Cu_2Se thin film prepared by a low-cost and scalable solution process. Benefiting from previously reported cosolvent approach that is capable of directly processing a variety of semiconductor solids,[34–37] Cu_2Se powder is readily dissolved in the mixture of ethylenediamine and ethanedithiol in several minutes at room temperature. The formulated Cu_2Se ink solution could be readily used to process smooth and crystalline thin film on Al_2O_3 or plastic substrates, via wet-deposition methods such as spin coating. The truly soluble precursor as the ink material leads to the improved structural perfection and thus delivers a higher electrical performance. The fabricated Cu_2Se thin film exhibits a power factor of 0.62 mW/(m K^2) at 684 K on rigid Al_2O_3 substrate and 0.46 mW/(m K^2) at 664 K on flexible polyimide substrate, which is considerably higher than those of solution processed Cu_2Se thin films (<0.1 mW/(m K^2)) reported previously and among the highest values achieved in all flexible thermoelectric films (≈0.5 mW/(m K^2)) to date. Furthermore, the Cu_2Se thin film shows excellent flexibility, with a resistance increase of only 8% and nearly unchanged thermal conductivity after 1000 bending cycles. The ultrafast optical spectroscopy reveals a thermal conductivity of 1.3-1.5 W/(m K) at room temperature which is comparable to that of the Cu_2Se in the pressed bulk form. The prepared flexible Cu_2Se thin film thermoelectric materials present an exciting advancement in flexible thermoelectrics for the next-generation flexible electronics and sensors.

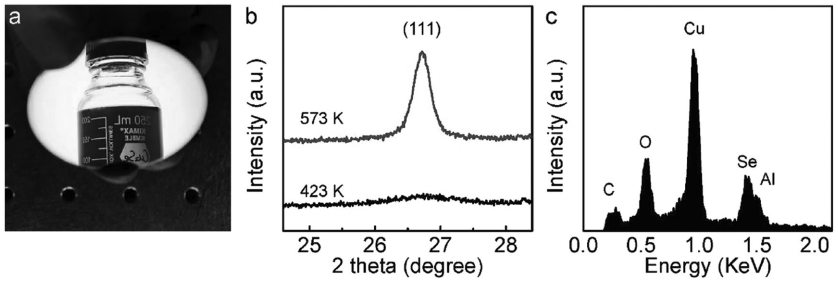

Figure 1. Characterization of the solution processed Cu_2Se thin film on Al_2O_3 substrate. a) Photograph of the deposited Cu_2Se thin film on a standard 2 inch *c*-plane Al_2O_3 substrate, showing a mirror-like reflection. b) X-ray diffraction (XRD) pattern of the film annealed at 423 and 573 K. c) Energy dispersive X-ray spectrum (EDS) of the film annealed at 573 K.

To prepare the Cu_2Se thin film, an ink solution is first formulated using a cosolvent approach by dissolving Cu_2Se powder in a mixture of ethylenediamine and ethanedithiol at room temperature. The ink solution could be coated onto different substrates, including SiO_2/Si, Al_2O_3, glass, and plastic, in a scalable fashion by using a spin coating or printing process. The coated substrate was next treated with thermal annealing to yield a pure phase of Cu_2Se thin film. For thermoelectric measurement, the continuous Cu_2Se thin film was spin coated on the Al_2O_3 substrate. The resulting film shows a high degree of uniformity over a large area with mirror-like reflection (**Figure 1**a), similar to previously reported smooth films.[35,38] X-ray diffraction (XRD) studies show that the as-coated film is not crystalline, which can be readily converted into highly crystalline thin film with a moderate thermal annealing at 573 K or higher (Figure 1b and Figure S1, Supporting Information). The energy dispersive X-ray spectral studies indicate a Cu/Se atomic ratio of 1.79 ± 0.06, 1.87 ± 0.06, 1.95 ± 0.07, and 1.96 ± 0.07 for the Cu_2Se thin film annealed at 573, 623, 703, and 773 K, respectively (Figure 1c). The elemental analyses suggest the considerable Cu deficiency in the resulting thin films, which is consistent with previous studies.[37] The increasing Cu/Se ratio with increasing annealing temperature can be attributed to the loss of Se at high temperature.

The scanning electron microscopic (SEM) studies (**Figure 2**a) suggest that the resulting thin film consists of compact ultrafine nanoparticles (≈10 nm), which is also confirmed by atomic force microscopy (AFM) analysis (Figure 2b). The as-prepared thin film on Al_2O_3 substrate shows a thickness of 55 nm and a surface roughness R_a = 3.1 nm (Figure 2b,c). The cross-sectional SEM image (Figure 2d) further confirms the relatively smooth thin film and demonstrates that the film is free of obvious voids. The high-resolution transmission electron microscopic (TEM) image of the cross-sectional view of the thin film (Figure 2e,f and Figure S2, Supporting Information)

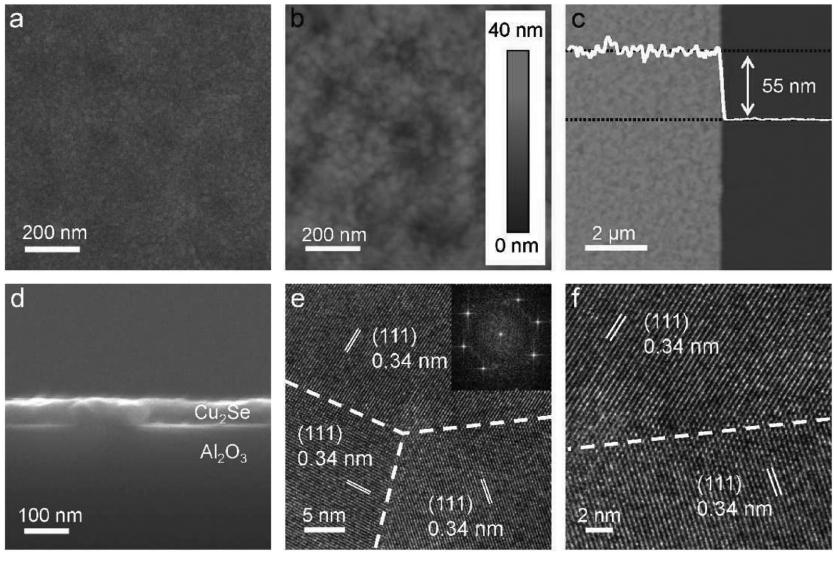

Figure 2. Structural characterization of the Cu_2Se thin films. a) Scanning electron microscopic (SEM) image of the surface of the film. b) Atomic force microscopy (AFM) analysis of the surface roughness and c) thickness of the film. d) Cross-sectional SEM analysis of the film on Al_2O_3 substrate. e) TEM analysis of the nanocrystals in the film. The dashed lines highlight the grain boundaries. Inset is the corresponding FFT of the TEM image. f) High resolution TEM image of the two nanocrystals in (e).

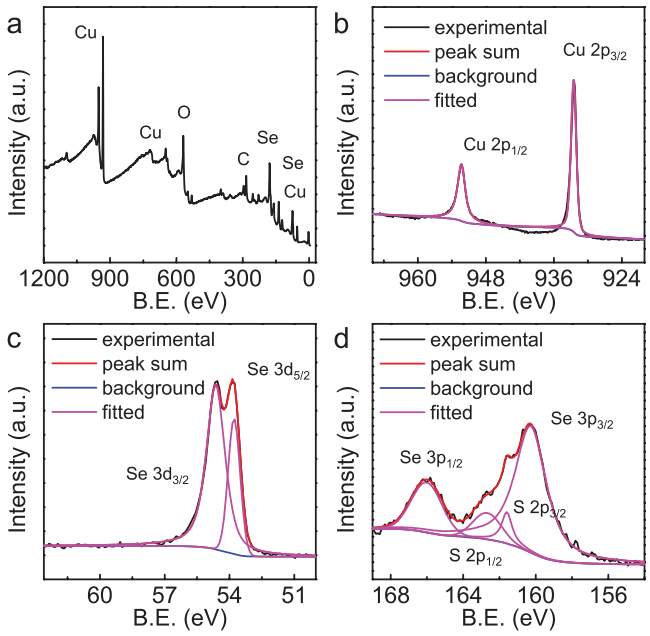

Figure 3. X-ray photoelectron spectroscopy analysis of the Cu_2Se thin film. a) Survey. b) Cu 2p. c) Se 3d. d) Se 3p and S 2p.

shows that the film is constructed of multiple crystalline nanoparticles that stack compactly with each other. The polycrystalline nature is further confirmed by three sets of spot in the corresponding fast Fourier transform (FFT) (inset in Figure 2e), indicating three nanocrystals with different orientation. The close contact and strong coupling between each crystalline grain, which essentially differs from that in the nanocrystal ink-based films, is expected to be beneficial for the electron transport across the interface which would enable excellent electrical performance.[39,40]

To further identify the elemental valence states and purity of the resulted film, the X-ray photoelectron spectroscopy (XPS) measurements were performed. The survey spectrum (**Figure 3**a) indicates the existence of both Cu and Se content. As illustrated in Figure 3b, the Cu 2p core level spectrum has two peaks (Cu $2p_{3/2}$ and $2p_{1/2}$) that are symmetric, narrow, and free of satellite peaks, indicating that the valences of Cu elements is pure +1.[35] As for Se 3d spectrum, a broad peak at 52–56 eV was observed (Figure 3c), which is the characteristic shape of Se^{2-} in a consistent bonding environment.[41–43] The broad peak for Se 3d can be fitted into two symmetric peaks to be assigned to Se $3d_{5/2}$ and Se $3d_{3/2}$, respectively. The XPS studies also reveal an atomic ratio for Cu/Se ranging from 1.8 to 2.0, suggesting the considerable Cu deficiency that can lead to the self-doping effect.[37] The S 2p peaks could be resolved although partially overlapping with the Se 3p double peaks. The existence of S might result from the ethanedithiol residue that was not fully removed during the thermolysis.[34,36] While XRD and EDS did not show detectable amount of S, it is likely that the overall S content is rather low and mainly concentrates on the surface of the film to give a more obvious signal in the surface sensitive XPS technique.

The in-plane Seebeck coefficient and electrical conductivity of Cu_2Se thin films were measured using a commercial Linseis Seebeck and resistivity instrument. **Figure 4** shows the temperature-dependent thermoelectric properties of four samples annealed at different temperatures ranging from 573 to 773 K, measured up to the corresponding annealing temperature to avoid any additional undesired structural change during the measurement. It is noted that the electrical conductivity decreases while the Seebeck coefficient grows higher with increasing temperature in all thin films (Figure 4a,b). In general, the carrier concentrations in all films are relatively high (Figure S3, Supporting Information), which also suggests that the Cu content is off stoichiometry as the self-doping effect. The higher annealing temperature leads to a reduced electrical conductivity and an improved Seebeck coefficient, which may be attributed to the decreasing carrier concentration (Figure S3a, Supporting Information). The Se content is prone to leave the film at high annealing temperature, as shown in our elemental analyses. The loss of Se content reduces the self-doping effect caused by the Cu deficiency and decreases the carrier (hole) concentration. Similar results were obtained in a recent study on the solution processed Cu_2Se thin film at room temperature, which initially demonstrated the potential of such material for thermoelectric applications.[37] Together, the combined power factor increases with the measured temperature and does not reach the peak (within our measurement range) that usually appears beyond 800 K.[29,44] This trend is similar to those observed in the previously reported Cu_2Se bulk pellets. Most significantly, the film annealed at 703 K was found to exhibit the highest power factor among the four samples, which is 0.62 mW/(m K^2) at 684 K (Figure 4c). Since the material and performance stability during the thermal cycle is an important parameter for the thermoelectric device, cycling test was performed on the prepared thin film which shows similar behavior to the typical Cu_2Se (Figure S4, Supporting

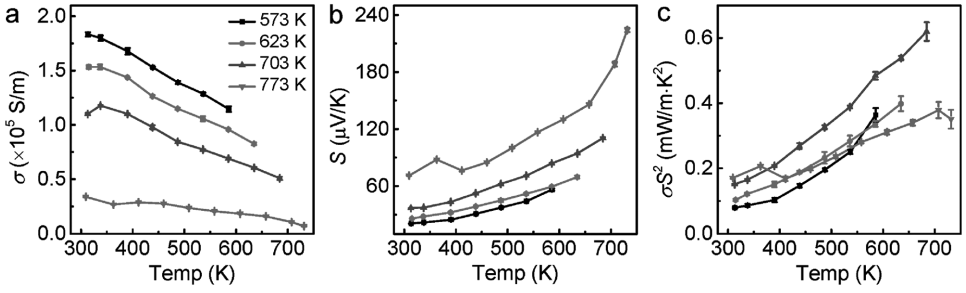

Figure 4. Thermoelectric properties of the solution processed Cu_2Se film on Al_2O_3 substrate annealed at various temperature. a) Electrical conductivity σ, b) Seebeck coefficient S, and c) power factor σS^2 of the film measured in the helium atmosphere.

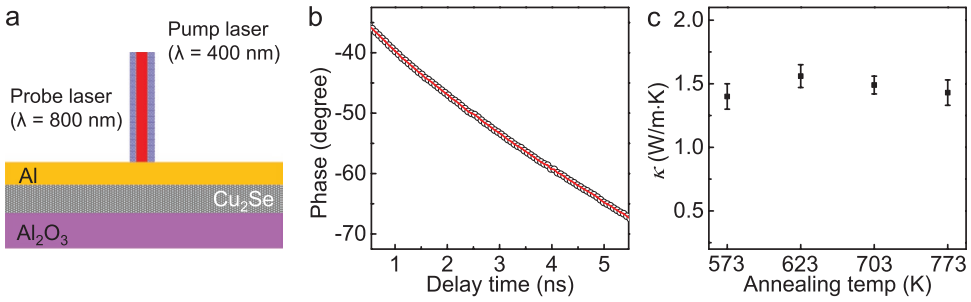

Figure 5. Thermal transport measurement of the Cu_2Se film using ultrafast optical spectroscopy. a) Schematic illustration of the measurement setup, showing the Al transducer film on the top, pump laser to heat the local area of the film and probe laser to monitor the thermoreflectance change. b) Normalized TDTR phase change versus time, fit by the diffusive model. Experimental curves (black circles) and the best fitting from the multilayer thermal transport model (red line). c) Thermal conductivity values measured in multiple samples annealed at different temperature. Error bars indicate the standard deviations from ten measurements.

Information). The superior thermoelectric performance is mainly attributed to the highly compact crystalline thin film with close contact between nanoparticles, which would result in excellent electron transport properties.[39,40] The truly soluble precursor as ink solution is proposed to be more effective to fabricate highly compact and void-free thin film thermoelectric devices, comparing with nanocrystal ink solution which forms the intrinsical void space within the film. Therefore, the cosolvent approach enables the production of thin film devices with higher structural perfection.

The thermal conductivity was measured using the time-domain thermoreflectance (TDTR) technique. TDTR is now a standard technique for measuring the thermal conductivity of a wide range of material.[45–47] In the measurement setup, a femtosecond pulse laser is split into a pump and a probe beam (**Figure 5**a and Note S1, Supporting Information). An instantaneous temperature rise on the sample surface is generated due to the pump laser impulses (λ = 400 nm), and the time-dependent temperature decay is monitored by the probe beam (λ = 800 nm). Such a transient decay curve is subsequently fit with a multilayer thermal model to obtain the thermal conductivity. Figure 5b shows typical TDTR data and fits to the thermal model. The best-fitted thermal conductivity values are plotted in Figure 5c for samples with different annealing temperatures. Thermal conductivity of the film slightly increases when the annealing temperature increases from 573 to 773 K. At room temperature, the thermal conductivity values of all films fall within the range between 1.3 and 1.5 W/(m K). Such thermal conductivity is comparable to the previously reported value for nanostructured bulk Cu_2Se[27,29,48] and indicates that our solution processed thin films retains the intrinsic thermal property of Cu_2Se material. By probing the temperature-dependent thermal conductivity, the *ZT* value in the whole measurement range could be calculated (Figure S5, Supporting Information) and is comparable to those of the high-temperature or high-pressure processed nanostructure-bulk Cu_2Se.

Importantly, our solution processed Cu_2Se thin films can be readily implemented on plastic substrate to create flexible thermoelectric thin films. The Cu_2Se thin film on polyimide substrate exhibits slightly lower thermoelectric performance (**Figure 6**a–c) than that on the rigid and highly smooth Al_2O_3 substrate. A power factor of 0.46 mW/(m K^2) at 664 K is obtained from Cu_2Se/polyimide. As far as we know, this value is much higher than those of other solution processed Cu_2Se thin films (<0.1 mW/(m K^2)) and among the highest ones in all flexible thermoelectric films (≈0.5 mW/(m K^2)) reported to date.[22,31–33] The relatively lower power factor may be largely attributed to the rougher surface for the films processed on plastic. In order to explore the potential application in flexible devices, we have performed the flexibility test on thin film deposited on the polyimide substrate (Figure 6d–f). The Cu_2Se film shows a resistance change of only 8% after 1000 bending cycles, in contrast to >600% resistance increase in a typical sputtered indium tin oxide (ITO) thin film (Figure 6e). At the same time, the thermal conductivity value displays a negligible change after 1000 bending cycles (Figure 6f). Together, the retention of superior thermoelectric performance after mechanical bending could be expected in the fabricated Cu_2Se thin film. The excellent flexibility is most desired for the integration with the flexible electronics and sensors for attaching to curved heating surfaces.

In summary, we have reported a high-performance thermoelectric thin film fabricated from a low-cost and scalable solution process. The ink solution was prepared by the direct dissolution of Cu_2Se powder into a cosolvent at room temperature. Smooth and void-free crystalline thin films on Al_2O_3 or plastic substrates could be readily obtained by a spin coating process. The resulted Cu_2Se thin film exhibits a power factor of 0.62 and 0.46 mW/(m K^2) on rigid Al_2O_3 and flexible polyimide substrate, respectively, which are much higher than values from other solution processed Cu_2Se thin films (<0.1 mW/(m K^2)) and among the highest ones in all the flexible thermoelectric films (≈0.5 mW/(m K^2)) reported to date. The structure perfection and superior electrical performance is mainly attributed to the ink solution with a truly soluble precursor, which is essentially different from the nanocrystal-based ink. The ultrafast optical spectroscopy reveals a room-temperature thermal conductivity of 1.3–1.5 W/(m K), comparable to that of the Cu_2Se in the pressed bulk form. Besides, the Cu_2Se thin film coated on plastic substrate shows a superior flexibility for the integration with flexible electronics. The low-cost and scalable fabrication process, together with a remarkable thermoelectric performance obtained in relatively earth-abundant elements, offers great opportunities in powering the next-generation flexible electronics and sensors.

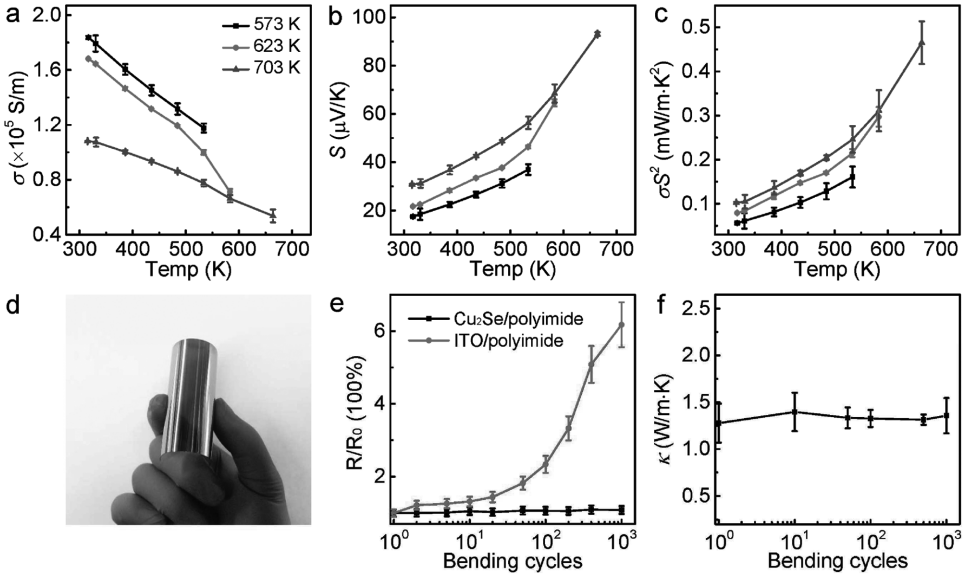

Figure 6. Thermoelectric performance of Cu_2Se thin film on flexible plastic substrate. a) electrical conductivity σ, b) Seebeck coefficient S, and c) power factor σS^2 of the film deposited on polyimide substrate. d) Photograph of the Cu_2Se thin film on the polyimide substrate. e) Relative resistance change of the Cu_2Se thin film on the polyimide substrate in response to the bending cycles for the 60 nm thick solution processed Cu_2Se thin film and 60 nm thick sputtered ITO thin film on polyimide substrate. f) Thermal conductivity change in response to the bending cycles. The bending radius is 10 mm and the tensile strain is 0.0025.

Experimental Section

Chemicals: Ethylenediamine ($H_2NCH_2CH_2NH_2$, >99%) and ethanedithiol ($HSCH_2CH_2SH$, >98+%) were purchased from Alfa-Aesar. Copper (I) selenide (Cu_2Se, >99.95%) was purchased from Sigma-Aldrich. All the chemicals were used as received without further purification.

Deposition of Cu_2Se Film on Al_2O_3 and Plastic Substrates: 50 mg of Cu_2Se powder was weighed and transferred to a glass vial. 2 mL ethylenediamine was added into the vial followed by the addition of 0.2 mL ethanedithiol in a nitrogen-filled glovebox. After 10 min of magnetic stirring, the complete dissolution of the powder indicated the formation of the ink solution. The gentle warming during the dissolution (e.g., 35 °C on hotplate) could facilitate the process. The substrates (Al_2O_3 and polyimide) were used after washing with isopropyl alcohol followed by a 5 min oxygen plasma treatment to increase the hydrophilicity of the substrate surface. A certain volume of ink solution was spin coated onto the substrate with a speed of 2000 rpm for 70 s. Then the coated substrate was heated on a hotplate at temperature between 300 and 500 °C (573–773 K) for 1 hr with a slow ramp. All of the above processes were performed in a nitrogen-filled glovebox.

Structural and Compositional Characterizations: Characterizations were carried out using scanning electron microscopy (SEM, JEOL JSM-6700F FE-SEM) with energy dispersive X-ray spectroscopy (EDAX), transmission electron microscopy (Titan S/TEM FEI; acceleration voltage, 300 kV), AFM (Bruker Dimension Icon Scanning Probe Microscope), XRD (Bruker D8 Discover Powder X-ray Diffractometer), and XPS (AXIS Ultra DLD). The cross-sectional sample was prepared by cutting the film on the Al_2O_3 substrate using focused ion beam.

Thermoelectric Measurement: The temperature-dependent in-plane electrical conductivity and Seebeck coefficient of the Cu_2Se films were measured simultaneously using a commercial Linseis Seebeck and resistivity instrument in a helium atmosphere. The resistivity measurement was conducted using a linear four-probe configuration. The Seebeck coefficient was determined by measuring the Seebeck voltage and the temperature difference established in parallel to the sample surface. The measurement uncertainties were less than 2% for the electrical conductivity and less than 3% for the Seebeck coefficient, respectively. The carrier concentration data on the thin films were collected with a PPMS (Physical Property Measurement System, Quantum Design) following the standard *van der Pauw* method.

Ultrafast Optical Spectroscopy: The Cu_2Se thin film was prepared on the Al_2O_3 or polyimide substrate, followed by the deposition of an 80 nm aluminum (Al) thin film using the electron-beam evaporator. Thermal transport was characterized using the TDTR technique. The basic setup was presented in ref. [40] and more details about the measurement could be found in Note S1 (Supporting Information). A tunable Ti:sapphire laser emitted a train of 100 fs pulses at a repetition rate of 80.7 MHz and a central wavelength of 800 nm. The light was divided into pump and probe beams by the first beam splitter, with a large power ratio between the two beams. The pump beam (with spot size of 50 μm) passed through an electro-optic modulator with a sine-wave modulation up to 20 MHz and then through a bismuth triborate (BIBO) crystal, where its frequency was doubled to 400 nm. The probe beam (with spot size of 10 μm) was controlled with a delay time delay (up to 6 ns) by a time-delay stage, and its reflected intensity was measured by a photodiode detector (Thorlabs PDA36A). The measurement on the sample at the elevated temperature was performed similarly by heating the Cu_2Se/Al_2O_3 using a thermal couple equipped with a temperature controller.

Supporting Information

Supporting Information is available from the Wiley Online Library or from the author.

Acknowledgements

Z.L., C.H., and J.S.K. contributed equally to this work. X.D. and Y.H. acknowledge the financial support from National Science FoundationEFRI-1433541. C.H. thanks the support from the National Science Foundation Graduate Research Fellowship Program under Grant No. 1545659. Y.J.H. acknowledges support from the Sustainable

LA Grand Challenge and the Anthony and Jeanne Pritzker Family Foundation.

Received: December 8, 2016
Revised: February 15, 2017
Published online: March 29, 2017

[1] L. E. Bell, *Science* **2008**, *321*, 1457.
[2] D. M. Rowe, *Thermoelectrics Handbook: Macro to Nano*, CRC Press, Boca Raton, FL, USA **2006**.
[3] J. R. Sootsman, D. Y. Chung, M. G. Kanatzidis, *Angew. Chem., Int. Ed.* **2009**, *48*, 8616.
[4] M. Zebarjadi, K. Esfarjani, M. S. Dresselhaus, Z. F. Ren, G. Chen, *Energy Environ. Sci.* **2012**, *5*, 5147.
[5] L. D. Hicks, M. S. Dresselhaus, *Phys. Rev. B* **1993**, *47*, 12727.
[6] Y. Wang, H. J. Fan, *J. Phys. Chem. C* **2010**, *114*, 13947.
[7] H. R. Yang, J. H. Bahk, T. Day, A. M. S. Mohammed, G. J. Snyder, A. Shakouri, Y. Wu, *Nano Lett.* **2015**, *15*, 1349.
[8] Y. C. Zhang, G. D. Stucky, *Chem. Mater.* **2014**, *26*, 837.
[9] T. C. Harman, P. J. Taylor, M. P. Walsh, B. E. LaForge, *Science* **2002**, *297*, 2229.
[10] F. J. Fan, B. Yu, Y. X. Wang, Y. L. Zhu, X. J. Liu, S. H. Yu, Z. F. Ren, *J. Am. Chem. Soc.* **2011**, *133*, 15910.
[11] H. Y. Fang, J. H. Bahk, T. L. Feng, Z. Cheng, A. M. S. Mohammed, X. W. Wang, X. L. Ruan, A. Shakouri, Y. Wu, *Nano Res.* **2016**, *9*, 117.
[12] K. Biswas, J. Q. He, I. D. Blum, C. I. Wu, T. P. Hogan, D. N. Seidman, V. P. Dravid, M. G. Kanatzidis, *Nature* **2012**, *489*, 414.
[13] B. Poudel, Q. Hao, Y. Ma, Y. C. Lan, A. Minnich, B. Yu, X. A. Yan, D. Z. Wang, A. Muto, D. Vashaee, X. Y. Chen, J. M. Liu, M. S. Dresselhaus, G. Chen, Z. F. Ren, *Science* **2008**, *320*, 634.
[14] R. Venkatasubramanian, E. Siivola, T. Colpitts, B. O'Quinn, *Nature* **2001**, *413*, 597.
[15] R. Tangirala, J. L. Baker, A. P. Alivisatos, D. J. Milliron, *Angew. Chem., Int. Ed.* **2010**, *49*, 2878.
[16] M. S. Dresselhaus, G. Chen, M. Y. Tang, R. Yang, H. Lee, D. Wang, Z. Ren, J.-P. Fleurial, P. Gogna, *Adv. Mater.* **2007**, *19*, 1043.
[17] D. Ding, D. Wang, M. Zhao, J. Lv, H. Jiang, C. Lu, Z. Tang, *Adv. Mater.* **2017**, *29*, 1603444.
[18] Y. Min, J. W. Roh, H. Yang, M. Park, S. II Kim, S. Hwang, S. M. Lee, K. H. Lee, U. Jeong, *Adv. Mater.* **2013**, *25*, 1425.
[19] Z. H. Wang, L. Yang, X. J. Li, X. T. Zhao, H. L. Wang, Z. D. Zhang, X. P. A. Gao, *Nano Lett.* **2014**, *14*, 6510.
[20] R. He, S. Sucharitakul, Z. P. Ye, C. Keiser, T. E. Kidd, X. P. A. Gao, *Nano Res.* **2015**, *8*, 851.
[21] F. Suarez, A. Nozariasbmarz, D. Vashaee, M. C. Ozturk, *Energy Environ. Sci.* **2016**, *9*, 2099.
[22] J. H. Bahk, H. Y. Fang, K. Yazawa, A. Shakouri, *J. Mater. Chem. C* **2015**, *3*, 10362.
[23] Y. N. Chen, Y. Zhao, Z. Q. Liang, *Energy Environ. Sci.* **2015**, *8*, 401.
[24] Y. Yang, Z. H. Lin, T. Hou, F. Zhang, Z. L. Wang, *Nano Res.* **2012**, *5*, 888.
[25] I. Hyeongwook, M. H. Geun, L. J. Seok, C. I. Young, K. T. June, K. Y. Hyup, *Nano Res.* **2014**, *7*, 443.
[26] X. Liu, Y. Z. Long, L. Liao, X. F. Duan, Z. Y. Fan, *ACS Nano* **2012**, *6*, 1888.
[27] H. L. Liu, X. Shi, F. F. Xu, L. L. Zhang, W. Q. Zhang, L. D. Chen, Q. Li, C. Uher, T. Day, G. J. Snyder, *Nat. Mater.* **2012**, *11*, 422.
[28] X. L. Su, F. Fu, Y. G. Yan, G. Zheng, T. Liang, Q. Zhang, X. Cheng, D. W. Yang, H. Chi, X. F. Tang, Q. J. Zhang, C. Uher, *Nat. Commun.* **2014**, *5*, 4908.
[29] B. Yu, W. S. Liu, S. Chen, H. Wang, H. Z. Wang, G. Chen, Z. F. Ren, *Nano Energy* **2012**, *1*, 472.
[30] H. L. Liu, X. Yuan, P. Lu, X. Shi, F. F. Xu, Y. He, Y. S. Tang, S. Q. Bai, W. Q. Zhang, L. D. Chen, Y. Lin, L. Shi, H. Lin, X. Y. Gao, X. M. Zhang, H. Chi, C. Uher, *Adv. Mater.* **2013**, *25*, 6607.
[31] A. Ghosh, C. Kulsi, D. Banerjee, A. Mondal, *Appl. Surf. Sci.* **2016**, *369*, 525.
[32] S. Deka, A. Genovese, Y. Zhang, K. Miszta, G. Bertoni, R. Krahne, C. Giannini, L. Manna, *J. Am. Chem. Soc.* **2010**, *132*, 8912.
[33] Y. Zhang, C. G. Hu, C. H. Zheng, Y. Xi, B. Y. Wan, *J. Phys. Chem. C* **2010**, *114*, 14849.
[34] D. H. Webber, R. L. Brutchey, *J. Am. Chem. Soc.* **2013**, *135*, 15722.
[35] Z. Y. Lin, Q. Y. He, A. X. Yin, Y. X. Xu, C. Wang, M. N. Ding, H. C. Cheng, B. Papandrea, Y. Huang, X. F. Duan, *ACS Nano* **2015**, *9*, 4398.
[36] D. H. Webber, J. J. Buckley, P. D. Antunez, R. L. Brutchey, *Chem. Sci.* **2014**, *5*, 2498.
[37] Y. Ma, P. B. Vartak, P. Nagaraj, R. Y. Wang, *RSC Adv.* **2016**, *6*, 99905.
[38] Z. Y. Lin, Y. Chen, A. X. Yin, Q. Y. He, X. Q. Huang, Y. X. Xu, Y. Liu, X. Zhong, Y. Huang, X. F. Duan, *Nano Lett.* **2014**, *14*, 6547.
[39] C. R. Kagan, C. B. Murray, *Nat. Nanotechnol.* **2015**, *10*, 1013.
[40] D. V. Talapin, J. S. Lee, M. V. Kovalenko, E. V. Shevchenko, *Chem. Rev.* **2010**, *110*, 389.
[41] S. L. Liu, Z. S. Zhang, J. C. Bao, Y. Q. Lan, W. W. Tu, M. Han, Z. H. Dai, *J. Phys. Chem. C* **2013**, *117*, 15164.
[42] S. C. Riha, D. C. Johnson, A. L. Prieto, *J. Am. Chem. Soc.* **2011**, *133*, 1383.
[43] J. B. Zhu, Q. Y. Li, L. F. Bai, Y. F. Sun, M. Zhou, Y. Xie, *Chem. Eur. J.* **2012**, *18*, 13213.
[44] L. L. Zhao, X. L. Wang, J. Y. Wang, Z. X. Cheng, S. X. Dou, J. Wang, L. Q. Liu, *Sci. Rep.* **2015**, *5*, 7671.
[45] A. J. Schmidt, X. Y. Chen, G. Chen, *Rev. Sci. Instrum.* **2008**, *79*, 114902.
[46] D. G. Cahill, *Rev. Sci. Instrum.* **2004**, *75*, 5119.
[47] Y. J. Hu, L. P. Zeng, A. J. Minnich, M. S. Dresselhaus, G. Chen, *Nat. Nanotechnol.* **2015**, *10*, 701.
[48] X. Q. Chen, Z. Li, S. X. Dou, *ACS Appl. Mater. Interfaces* **2015**, *7*, 13295.